

MoQuad: Motion-focused Quadruple Construction for Video Contrastive Learning

Yuan Liu¹†, Jiacheng Chen²†, and Hao Wu³

¹ The University of Hong Kong

² Simon Fraser University

³ Bytedance Inc

Abstract. Learning effective motion features is an essential pursuit of video representation learning. This paper presents a simple yet effective sample construction strategy to boost the learning of motion features in video contrastive learning. The proposed method, dubbed **M**otion-focused **Q**uadruple Construction (MoQuad), augments the instance discrimination by meticulously disturbing the appearance and motion of both the positive and negative samples to create a quadruple for each video instance, such that the model is encouraged to exploit motion information. Unlike recent approaches that create extra auxiliary tasks for learning motion features or apply explicit temporal modelling, our method keeps the simple and clean contrastive learning paradigm (*i.e.*, SimCLR) without multi-task learning or extra modelling. In addition, we design two extra training strategies by analyzing initial MoQuad experiments. By simply applying MoQuad to SimCLR, extensive experiments show that we achieve superior performance on downstream tasks compared to the state of the arts. Notably, on the UCF-101 action recognition task, we achieve 93.7% accuracy after pre-training the model on Kinetics-400 for only 200 epochs, surpassing various previous methods.

Keywords: video representation learning, contrastive learning

1 Introduction

The recent progress of self-supervised visual representation learning has provided exciting opportunities for exploiting the huge amount of unlabelled web images and videos to train extremely powerful neural networks. In the image domain, seminal works based on contrastive learning (*e.g.*, SimCLR [7], MoCo [20]) have largely closed the performance gap between self-supervised learning methods and the supervised learning counterparts across various downstream tasks. However, the progress in the video domain lags behind as videos contain rich motion information, making the learning of video representations more challenging.

†Work done when interned at Bytedance Inc.

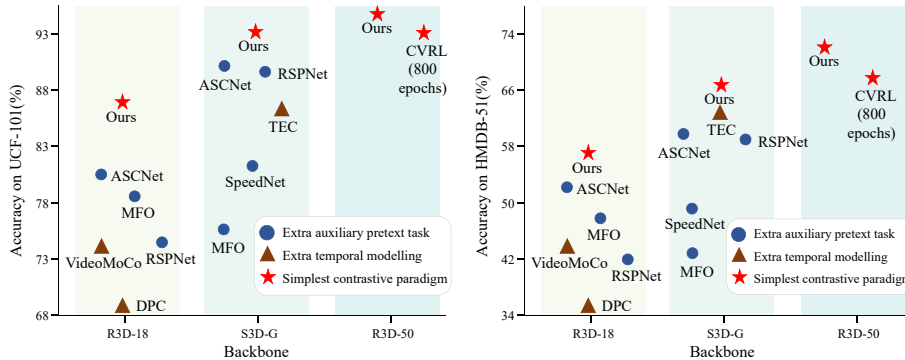


Fig. 1. Performance of MoQuad on UCF-101 and HMDB-51 action recognition (transfer learning pre-trained on Kinetics-400 [5] for only 200 epochs) with different video backbones, compared to other video self-supervised learning methods. The full results corresponding to this figure are available in Table 1.

Contrastive learning is still an effective framework for video self-supervised learning [12,38], but to further encourage the learning of motion-oriented features, extra designs are usually needed. For example, RspNet [6], ASCNet [23] and Pace [40] propose an extra motion branch and conduct multi-task learning, while DPC [16], MemDPC [16] and VideoMoCo [36] apply explicit temporal modeling for better modeling motion information.

This paper aims to keep the simplest video contrastive learning paradigm (*i.e.*, single-task, no extra modelling), but significantly improve the learning of motion features. Our main contribution is a carefully designed sample construction strategy that enriches the vanilla instance discrimination and enforces the model to capture effective motion information to finish the discrimination task.

Concretely, for each anchor clip, the instance discrimination [12] task requires the model to pull clips from the same video instance (positive sample) closer while pushing clips from different instances (negative sample) apart. Our method then builds upon three progressive analyses:

- (1) Positive clip pairs from the same video instance share similar appearance and motion features, but ConvNets tend to excessively exploit the appearance clues (*e.g.*, background) to hack the instance discrimination task, thus neglecting the motion features [41]. To prevent the model from overly relying on the appearance clues, it is necessary to disturb the appearance of the positive sample.
- (2) However, compared to the negative samples from other videos, the appearance disturbed positive sample still shares higher similarity with the anchor in terms of the appearance, thus still leaving space for the model to bypass the motion feature. To alleviate this, we argue that an intra-video negative sample is further needed, which has exactly the same appearance information as the anchor, but with the motion feature being disturbed.
- (3) To distinguish the appearance-disturbed positive sample from the motion-disturbed intra-video negative sample, there exist two ways: learning ef-

fective motion features or hacking the bias introduced by the appearance disturbing operation. To completely block the latter option, we propose to further include one more intra-video negative sample by disturbing both the appearance and motion information.

Combining these three arguments, our method, **Motion-focused Quadruple Construction (MoQuad)**, creates a quadruple for each video instance consisting of 1) an anchor, 2) an appearance-disturbed positive sample, 3) a motion-disturbed intra-video negative sample, and 4) a motion-and-appearance-disturbed intra-video negative sample, and follows the standard contrastive learning paradigm to train the model. We also conduct detailed analyses to determine the appropriate disturbing operations for motion and appearance.

By simply applying MoQuad to SimCLR, experiments show that we considerably improve the transfer learning performance. In addition, by analyzing the initial MoQuad experiments, we further derive two training strategies that bring consistent improvements: 1) a warm-up strategy that warms up the model with an appearance-focused instance discrimination task, such that the model can concentrate more on learning motion features when training with MoQuad and being less distracted by appearance information; and 2) a hard negative sample mining strategy that pushes the model to better discriminate videos with potentially similar motion types.

Without any multi-tasking learning or extra temporal modelling, MoQuad surpasses state-of-the-art video self-supervised learning methods on various downstream tasks, including action recognition and video retrieval, with shorter pre-training schedules (See Fig. 1). Extensive ablation studies and analyses further justify the effectiveness of different components of our method.

2 Related Work

Self-supervised image representation learning Self-supervised image representation learning has become a hot topic in recent years. Previous studies focus on creating pretext tasks explicitly, such as predicting the rotation angle of an image [13], solving a jigsaw puzzle task [34] and solving a relative patch predicting task [47]. Recently, some works optimize clustering and representation learning jointly [45,29,4], or learning image visual representation by discriminating instances from each other through contrastive learning. [7] pulls two augmented crops from the same images together while pushing crops from different images apart, using InfoNCE [35]. [42] proposes to use a memory bank to store all image representations. To keep the representations consistent, [20] proposes MoCo, which stores image embeddings from a momentum update encoder in a queue and achieves superior performance. The above-mentioned methods usually rely on a large number of negative samples. Meanwhile, BYOL [15] and Siamese [8] learn meaningful representations by only maximizing the similarity of two augmented positive samples without using any negative samples.

Self-supervised video representation learning Similar to image- representation learning approaches, some video representation learning approaches cre-

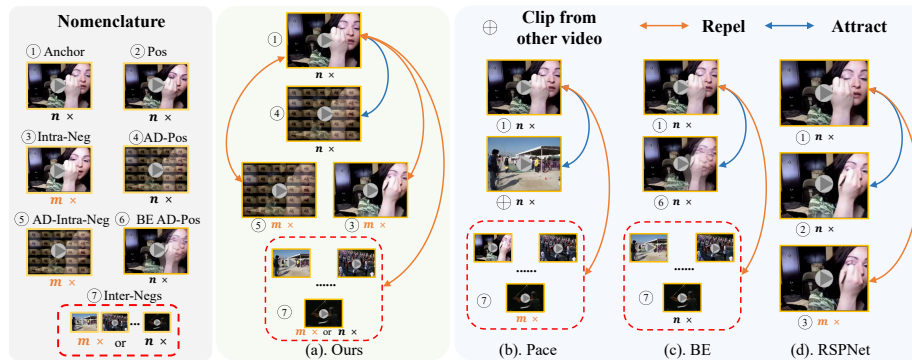


Fig. 2. Comparison between MoQuad with other motion-focused tasks from previous methods. (a): MoQuad, (b): motion task of Pace [40], (c): motion task of BE [41], (d): motion task of RSPNet [6]. $n \times$ and $m \times$ denote different video playback speeds. We disturb the appearance of the positive sample to create the appearance-disturbed positive sample and introduce two intra-video negative samples, one with motion disturbed and the other with both motion and appearance disturbed. Inter-Negs are clips from other videos. Please see Sec. 3.1 for full details.

ate pretext tasks [1,9,10,25,26,31,22]. Recently, contrastive learning becomes the mainstream in self-supervised video representation learning [38,16,17,18]. For example, CVRL [38] pulls two augmented clips from the same video together while pushing clips from different videos apart. Since the motion information is very important in videos, some approaches, *e.g.* [41], focus on extracting the motion of videos by preventing the model from focusing on the appearance. To extract both the motion and appearance information of videos, [6,40,23] propose to create two branches and achieve satisfactory results.

3 Method

Our method consists of 1) the MoQuad sample construction strategy, which is the key innovation of the paper (Sec 3.1), and 2) two extra training strategies derived by analyzing our initial experiments with MoQuad (Sec 3.2).

3.1 MoQuad sample construction

Definition of the motion-focused quadruple. Following the three-step analyses in Sec.1, MoQuad creates a quadruple from each video instance by carefully disturbing the motion and appearance information, aiming to enforce the learning of effective motion features. Given a video V_i , the quadruple consists of:

- An anchor (Anchor): a clip randomly sampled from V_i , denoted as A_i .
- An appearance-disturbed positive sample (AD-Pos): a clip randomly sampled from V_i , but with its appearance disturbed, denoted as \bar{P}_i .

- An intra-video negative sample (Intra-Neg): a clip randomly sampled from V_i , but with its motion information disturbed, denoted as N_i .
- An appearance-disturbed Intra-Neg (AD-Intra-Neg): a clip randomly sampled from V_i , but with both motion and appearance disturbed, denoted as \bar{N}_i .

We create the quadruple for each video in a batch, and clips from other videos serve as the inter-video negative samples (Inter-Negs) for the Anchor.

Instance discrimination with MoQuad. We pass A_i , \bar{P}_i , N_i , and \bar{N}_i to the feature extractor F and projection head H to get the clip features, denoted as z_{iA} , \bar{z}_{iP} , z_{iN} , and \bar{z}_{iN} , respectively. All the clip features are normalized. The vanilla instance discrimination task is augmented with per-instance quadruple:

$$L_m = - \sum_{i=0}^{B-1} \log \frac{\exp(z_{iA} \bar{z}_{iP} / \tau)}{\exp(z_{iA} \bar{z}_{iP} / \tau) + \sum S_{\text{Intra}} + \sum S_{\text{Inter}}} \quad (1)$$

τ is the temperature and B is the batch size. We use S_{Intra} and S_{Inter} to denote $\{\exp(z_{iA} z_{iN} / \tau), \exp(z_{iA} \bar{z}_{iN} / \tau)\}$ and $\{\exp(z_{iA} z_j / \tau)\}_{j \neq i}$, respectively. Note that z_j includes z_{jA} , \bar{z}_{jP} , z_{jN} and \bar{z}_{jN} , where i and j are the indices of two different videos.

Criteria for choosing disturbing operations. Determining the concrete disturbing operations is a key step to complete the design of MoQuad, and we first set up the desiderata for them:

- Appearance: The appearance disturbing operation is to augment the positive samples (AD-Pos). It should inject sufficiently strong noise into the video clip on the premise of preserving the original motion information, such that the model can be pushed hard to learn motion-focused features. Note that this operation is also applied to AD-Intra-Neg to prevent the model from hacking the bias introduced by the operation (See the analyses in Sec. 1).
- Motion: The motion disturbing operation is to augment the negative samples (*i.e.*, Intra-Neg and AD-Intra-Neg). In contrast to the appearance disturbing operation, it should only introduce subtle change to the motion information of a clip to make sure that the discrimination task cannot be trivially solved by the model. Similar arguments are also discussed in [3].

With these criteria, we are now ready to choose the disturbing operations.

Appearance disturbing operation. Appearance information contains both low and high-frequency information. BE [41] (Fig. 3(a)) provides an off-the-shelf operation by adding to each video frame a noise image randomly picked from the current video. However, this operation still keeps most of the high-frequency information of the original video and is not aggressive enough according to our criteria. To break both the low and high-frequency signals and make the operation stronger, we propose a simple improvement for constructing the noise image. Given a video V_i , we create an empty noise image (with the same shape as V_i), denoted as D . We then slice D into $k \times k$ windows (we use $k = 5$), and randomly sample a frame from another video to replace each empty window in D . We insert this noise image D to each frame of V_i by a weighted average of $\bar{V}_i = (1 - \lambda)V_i + \lambda D$. Fig. 3(c) illustrates this operation, and we name it as Repeated Appearance Disturbance (RAD). Note that the repeated frame can be



Fig. 3. Appearance disturbing operations. (a) the operation from BE [41], (b) RAD with the noise image from the current video (intra), and (c) RAD with noise image extracted from another video (inter).

sampled from the current video(Fig. 3(b)), but then it only introduces redundant signals to V_i and the RAD (intra) is not as strong as RAD (inter).

Motion disturbing operation. The motion information in videos can be generally represented as the temporal gradients [41]. There are three common approaches to disturb the temporal information of a video in the literature [6,27,33]: 1) change the playback speed (Speed), 2) reverse the frame order (Reverse), or 3) shuffle the frame order (Shuffle). Based on our criteria above, Reverse and Shuffle could change the motion information too much, thus making the negative samples trivial to be discriminated by the model. On the contrary, Speed only modifies the motion information subtly and is a more appropriate choice for MoQuad. To be more concrete, given a video V_i , we extract two clips C_i^n and C_i^m with dilation rate n and m , respectively. C_i^m and C_i^n are considered as an Intra-Neg for each other. With all operations determined, Fig. 2(a) is an illustration for the instance discrimination task with MoQuad quadruples.

Relation to previous methods. Pace [40], RspNet [6] and BE [41] are related previous methods that construct extra samples to improve the learning of motion feature for instance discrimination. All of them demonstrate different properties with MoQuad, and we make an illustrative comparison in Fig. 2.

Pace (Fig. 2(b)) enforces the model to pull clips of the same playback speed closer, no matter if these clips are from the same video or not. RspNet (Fig. 2(d)) argues that it is inappropriate to compare the speed of clips of different videos, thus only requiring the model to distinguish the playback speed of clips from the same video. Both Pace and RspNet add an extra speed-discrimination task to the contrastive learning framework. However, distinguishing the speed requires the model to focus more on low-level motion features (*e.g.*, the scale of the temporal gradients), and the model could fail to capture high-level motion semantics (*e.g.* motion types) without other negative samples. BE (Fig. 2(c)) does not use any extra auxiliary task. Instead, it breaks the appearance information of the positive sample to alleviate the negative impact of background bias [41]. However, as we analyzed and visualized above, its disturbing operation keeps most of the original appearance clues in the positive sample, and the model might still bypass the learning of effective motion features.

MoQuad (Fig. 2(a)) does not suffer from the potential issues of these methods. Compared to Pace and RspNet, we consider playback speed as a way to disturb the motion feature of Intra-Neg, instead of making it the only discrimi-

nation target (*i.e.*, our Inter-Negs can have the same speed but different motion type as the Anchor). Compared to BE, we employ stronger appearance disturbance by RAD and create extra motion-disturbed negative samples to further prevent the model from bypassing the learning of motion features.

3.2 Extra training strategies for MoQuad

In this section, we will introduce the two extra training strategies.

Appearance task warm-up. When training with MoQuad, the model exhibits two-stage learning progress: it starts with learning appearance-oriented features and gradually shifts to capture motion-oriented features (visualization in Fig. 4(left)), suggesting that the learning of appearance and motion can be better disentangled. Inspired by this discovery, we propose to use an appearance-focused task to warm up the model before training with MoQuad. We thus borrow the appearance task from RspNet [6] directly use it as the warm-up task. With the warm-up, MoQuad focuses on learning motion features from the very beginning of the training and learns better motion features (Fig. 4(right)). Algorithm 1 details the training schedule with the appearance task warm-up. The appearance task is simply an adapted instance discrimination task:

Given a batch of videos $\mathbf{V}_B = \{V_i\}_{i=0}^{B-1}$, for each video V_i in \mathbf{V}_B , we extract two clips with dilation n and m respectively, denoted as C_i^n and C_i^m . We pass C_i^n and C_i^m to feature extractor F and projection head H to get the features, and normalize these features to get the final feature vectors: z_i^n and z_i^m . The InfoNCE loss [35] again pulls clips from the same video together while pushing clips from different videos apart:

$$L_a = - \sum_{i=0}^{B-1} \log \frac{\exp(z_i^n z_i^m / \tau)}{\exp(z_i^n z_i^m / \tau) + \sum_{i \neq j, s \in \{n, m\}} \exp(z_i^n z_j^s / \tau)} \quad (2)$$

Hard negative sample mining. By visualizing the instance discrimination results of MoQuad, we find that the model sometimes has difficulty in distinguishing the positive samples from hard Inter-Negs. These hard inter-video negative samples turn out to share similar motion semantics as the Anchor (please check the Supplementary for the visualization and more analyses). Based on this observation, we propose a hard negative sample mining strategy to enforce the model to push these hard Inter-Negs farther away from the Anchor. For all the $\exp(z_{iA} z_j / \tau)$ in Eq. 1, we first get the top- K elements by:

$$S_{\text{Topks}} = \text{TopK}(\{\exp(z_{iA} z_j / \tau)\}_{i \neq j}) \quad (3)$$

where $K = \beta \times \text{len}(\{\exp(z_{iA} z_j / \tau)\}_{i \neq j})$ and β is the percentage of the total negative samples that are treated as hard negatives. We then assign a large weight, $\alpha (\alpha > 1)$, to these hard negative samples, and augment Eq. 1 by:

$$L_m = - \sum_{i=0}^{B-1} \log \frac{\exp(z_{iA} \bar{z}_{iP} / \tau)}{\exp(z_{iA} \bar{z}_{iP} / \tau) + \alpha \sum S_{\text{Intra}} + \alpha \sum S_{\text{Topks}} + \sum S_{\text{Easy}}} \quad (4)$$

For notation simplicity, S_{Easy} is defined as $S_{\text{Easy}} = S_{\text{Inter}} - S_{\text{Topks}}$ where $-$ is the difference between two sets.

Algorithm 1 Two-Stage Training Mechanism

Require: video set V , feature extractor F , projection head H , total epochs E , current epoch e and the percentage of total epochs p , used for the appearance task.

- 1: Initialize $e \leftarrow 0$
 - 2: // *Appearance Task Warmup*
 - 3: **while** $e < p \times E$ **do**
 - 4: Sample a batch of videos $V_B = \{V_i\}_{i=0}^{B-1}$ from video sets V .
 - 5: For each video in V_B , we extract two clips, C_i^n and C_i^m .
 - 6: Pass these clips to F and H to get z_i^n and z_i^m .
 - 7: Use Eq.2 to finish the instance discrimination task.
 - 8: $e \leftarrow e + 1$
 - 9: **end while**
 - 10: // *Instance Discrimination with MoQuad quadruple*
 - 11: **while** $p \times E \leq e < E$ **do**
 - 12: Sample a batch of videos $V_B = \{V_i\}_{i=0}^{B-1}$ from video sets V .
 - 13: For each video in V_B , we create the quadruple: A_i, \bar{P}_i, N_i and \bar{N}_i
 - 14: Pass $A_i, \bar{P}_i, N_i, \bar{N}_i$ to F and H to get $z_{iA}, \bar{z}_{iP}, z_{iN}$ and \bar{z}_{iN} .
 - 15: Use Eq.1 to finish the instance discrimination task.
 - 16: $e \leftarrow e + 1$
 - 17: **end while**
-

4 Experiments

We first describe the experimental setups in Sec. 4.1, including the datasets, pre-training details, evaluation settings, *etc.* In Sec. 4.2, we compare MoQuad with the state of the arts on two downstream tasks: action recognition and video retrieval. We then provide ablation studies in Sec. 4.3 to validate different design choices. In Sec. 4.4, we further present additional analyses to help understand the effectiveness of our method.

4.1 Experimental settings

Datasets. Four video action recognition datasets are covered in our experiments: Kinetics-400 (K400) [5], UCF101 [39], HMDB51 [30] and Something-Something-V2 (SSv2) [14]. K400 consists of 240K training videos from 400 human action classes, and each video lasts about 10 seconds. UCF101 contains 13,320 YouTube videos from 101 realistic action categories. HMDB51 has 6,849 clips from 51 action classes. SSv2 provides 220,847 videos from 174 classes and the videos contain more complex action information compared to UCF101 and HMDB51.

Self-supervised pre-training. There are various pre-training settings in the literature, we follow the same hyper-parameter choices as CVRL [38], including the image resolution (224×224) and the number of frames per clip (16). We evaluate our method with three different backbones: R3D-18 [19], S3D-G [43], and R3D-50 [38], so that we can compare with various previous works that use backbones with different model size. When pre-trained on K400, SSv2, and UCF101, the model is trained for 200, 200, and 800 epochs, respectively, which

follows the most common pre-training schedule in the literature [6,22,38,40]. Due to limited computational resources, we conduct ablation studies by pre-training the small R3D-18 backbone on UCF101 by default, unless otherwise specified. We use LARS [46] as our optimizer with a mini-batch of 256, which is consistent with SimCLR [7]. The learning rate is initialized to 3.2, and we use a half-period cosine learning rate decay scheduling strategy [21]. For appearance disturbing, we set $k = 5$ and uniformly sample λ from $[0.1, 0.5]$. For the warmup with appearance task, the appearance task takes up the first 20% of the training epochs. β and α are set to be 0.01 and 1.5 respectively for the hard negative sample mining.

Supervised fine-tuning for action recognition. Consistent with previous works [23,38,16], we fine-tune the pre-trained models on UCF101 or HMDB51 for 100 epochs and report the accuracy of action recognition. We sample 16 frames with dilation of 2 for each clip. The batch size is 32, and we use LARS [46] as the optimizer. The learning rate is 0.08, and we employ a half-period cosine learning rate decay strategy.

Linear evaluation protocol for action recognition. We also evaluate the video representations with the standard linear evaluation protocol [38]. We sample 32 frames for each clip with a temporal stride of 2 from each video. The linear classifier is trained for 100 epochs.

Evaluation details for action recognition. For computing the accuracy of action recognition, we follow the common evaluation protocol [11], which densely samples 10 clips from each video and employs a 3-crop evaluation. The softmax probabilities of all the 10 clips are averaged for each video to get the final classification results.

4.2 Comparison with state of the arts

We compare MoQuad with state-of-the-art self-supervised learning approaches on action recognition and video retrieval.

Evaluation on action recognition. As presented in Table 1, we compare our method with state of the arts under various experimental setups, with UCF101 and HMDB51 as the downstream datasets. Our method always outperforms the previous works with a clear margin when given the same pre-training settings. We note that even without the two extra training strategies, the vanilla MoQuad is still superior to previous methods.

As mentioned in Sec 4.1, UCF101 and HMDB51 are relatively small-scale datasets. To strengthen the comparison results, we further evaluate our model with the linear evaluation protocol on K400 and SSv2 datasets (Table 2). Our method can still consistently outperform previous works even with smaller effective batch size (*i.e.*, the number of different video instances in a batch).

Evaluation on video retrieval. We evaluate the learned video representation with nearest neighbour video retrieval. Following previous works [6,40], we sample 10 clips for each video uniformly and pass them to the pre-trained model to

Table 1. Action recognition results on UCF101 and HMDB51. We report the fine-tuning results of MoQuad and various baselines under different setups. MoQuad [†] is our method with the two extra training strategies. ⁸⁰⁰: pre-trained for 800 epochs, which is longer than the standard training schedule (*i.e.*, 200 epochs).

Method	Dataset	Backbone	Frame	Resolution	UCF101	HMDB51
CoCLR [18] ₂₀₂₀	UCF101	S3D	32	128	81.4	52.1
BE [41] ₂₀₂₁	UCF101	R3D-34	16	224	83.4	53.7
MoQuad (Ours)	UCF101	R3D-18	16	224	80.9	51.0
MoQuad [†] (Ours)	UCF101	R3D-18	16	224	82.7	53.0
MoQuad [†] (Ours)	UCF101	S3D-G	16	224	87.4	57.3
Pace [40] ₂₀₂₀	K400	R(2+1)D	16	112	77.1	36.6
MemoryDPC [17] ₂₀₂₀	K400	R3D-34	40	224	86.1	54.5
BE [41] ₂₀₂₁	K400	R3D-34	16	224	87.1	56.2
CMD [24] ₂₀₂₁	K400	R3D-26	16	112	83.7	55.2
DPC [16] ₂₀₁₉	K400	R3D-18	40	224	68.2	34.5
VideoMoCo [36] ₂₀₂₁	K400	R3D-18	32	112	74.1	43.1
RSPNet [6] ₂₀₂₁	K400	R3D-18	16	112	74.3	41.8
MFO [37] ₂₀₂₁	K400	R3D-18	16	112	79.1	47.6
ASCNet [23] ₂₀₂₁	K400	R3D-18	16	112	80.5	52.3
MoQuad (Ours)	K400	R3D-18	16	224	85.6	56.2
MoQuad [†] (Ours)	K400	R3D-18	16	224	87.3	57.7
MFO [37] ₂₀₂₁	K400	S3D	16	112	76.5	42.3
CoCLR [18] ₂₀₂₀	K400	S3D	32	128	87.9	54.6
SpeedNet [2] ₂₀₂₀	K400	S3D-G	64	224	81.1	48.8
RSPNet [6] ₂₀₂₁	K400	S3D-G	64	224	89.9	59.6
TEC [28] ₂₀₂₁	K400	S3D-G	32	128	86.9	63.5
ASCNet [23] ₂₀₂₁	K400	S3D-G	64	224	90.8	60.5
MoQuad (Ours)	K400	S3D-G	16	224	91.9	64.7
MoQuad [†] (Ours)	K400	S3D-G	16	224	93.0	65.9
CVRL [38] ₂₀₂₀ ⁸⁰⁰	K400	R3D-50	16	224	92.9	67.9
MoQuad (Ours)	K400	R3D-50	16	224	93.0	66.9
MoQuad [†] (Ours)	K400	R3D-50	16	224	93.7	68.0
MoQuad [†] ⁸⁰⁰ (Ours)	K400	R3D-50	16	224	94.7	71.5

get the clip features. Then, we apply average-pooling over the 10 clips to get the video-level feature vector. We use each video in the test split as the query and look for the k nearest videos in the training split of UCF101. The feature backbone is R3D-18, and the model is pre-trained on UCF101. The top- k retrieval accuracy ($k = 1, 5, 10$) is the evaluation metric. As in Table 3, we outperform previous methods consistently on all three metrics. Note that the gap between our method and recent work, ASCNet [23], is small, especially considering ASCNet has a smaller resolution. However, we do outperform ASCNet in Table 1 under the same experimental settings (*i.e.*, resolution 224, pre-trained on K400, and S3D-G backbone). A potential explanation is that fine-tuning could maximize the benefits of MoQuad.

Table 2. Action recognition results on two large-scale datasets. We further provide linear evaluation results on K400 and SSv2 to demonstrate the effectiveness of our method. Following the two recent works: CVRL [38] and COP_f [22], a R3D-50 backbone is pre-trained on the training split of the corresponding dataset for 200 epochs before conducting the standard linear evaluation. *: our re-implemented version.

Method	Backbone	Frame	Batch Size	Resolution	Linear eval.
Pre-trained and evaluated on K400 dataset					
CVRL [38] ₂₀₂₁	R3D-50	16	512	224	62.9
COP _f [22] ₂₀₂₁	R3D-50	16	512	224	63.4
MoQuad (Ours)	R3D-50	16	256	224	64.4
Pre-trained and evaluated on SSv2 dataset					
CVRL [38] ₂₀₂₁ *	R3D-50	16	256	224	31.5
COP _f [22] ₂₀₂₁	R3D-50	16	512	224	41.1
MoQuad (Ours)	R3D-50	16	256	224	44.0

Table 3. Evaluation on the video retrieval task.

Method	Backbone	Frame	Resolution	Top- <i>k</i>		
				<i>k</i> = 1	<i>k</i> = 5	<i>k</i> = 10
ClipOrder [44] ₂₀₁₉	R3D-18	16	112	14.1	30.3	40.0
SpeedNet [2] ₂₀₂₀	S3D-G	64	224	13.0	28.1	37.5
MemDPC [17] ₂₀₂₀	R(2+1)D	40	224	20.2	40.4	52.4
VCP [32] ₂₀₁₉	R3D-18	16	112	18.6	33.6	42.5
Pace [40] ₂₀₂₀	R(2+1)D	16	224	25.6	42.7	51.3
CoCLR-RGB [18] ₂₀₂₀	S3D-G	32	128	53.3	69.4	76.6
RSPNet [6] ₂₀₂₁	R3D-18	16	112	41.1	59.4	68.4
ASCNet [23] ₂₀₂₁	R3D-18	16	112	58.9	76.3	82.2
MoQuad (Ours)	R3D-18	16	224	60.8	77.4	83.5

4.3 Ablation studies

This subsection provides ablation studies for different design choices of the paper. As described in Sec. 4.1, all ablation experiments use an R3D-18 backbone due to the limited computational resources and a large number of trials.

The design of quadruple. We validate the effectiveness of each component of our quadruple in Table 4. We use SimCLR [7] as the base method and progressively add the elements of the quadruple. Both the fine-tuning and linear evaluation results are reported for UCF101 and HMDB51. Regardless of the pre-training dataset, each element of MoQuad quadruple improves the performance consistently. We would like to point out that K400 is much larger than UCF101 (see Sec. 4.1 for dataset stats), indicating that the benefits of our method do not degenerate as the size of the pre-training dataset grows.

The choice of disturbing operations. We present the results of different motion and appearance disturbing operations in Table 5. The left sub-table

Table 4. Ablation studies for components of MoQuad quadruple. We pre-train the R3D-18 backbone on UCF101 and K400, respectively. The fine-tuning and linear evaluation results on UCF101 and HMDB51 are reported.

AD-Pos	Intra-Neg	AD-Intra-Neg	Fine-tuning		Linear eval.	
			UCF	HMDB	UCF	HMDB
Pre-trained on UCF101 dataset						
-	-	-	76.0	44.3	68.8	33.6
✓	-	-	78.2	47.2	70.0	37.0
✓	✓	-	79.6	49.3	71.5	38.8
✓	✓	✓	80.9	51.0	73.9	40.3
Pre-trained on K400 dataset						
-	-	-	80.9	50.2	75.0	44.3
✓	-	-	82.1	53.6	76.2	47.4
✓	✓	-	84.5	55.0	77.3	48.4
✓	✓	✓	85.6	56.2	79.2	50.1

Table 5. Ablation studies for the disturbing operations. (Left) Different appearance disturbing operations. **(Right)** Different motion disturbing operations. The models are pre-trained on UCF101 for 800 epochs.

Operations	Fine-tuning		Linear eval.		Operations	Fine-tuning		Linear eval.	
	UCF	HMDB	UCF	HMDB		UCF	HMDB	UCF	HMDB
BE [41]	79.7	48.5	71.8	39.4	Reverse	76.3	45.4	69.8	34.7
RAD (Intra)	80.1	49.0	72.0	39.4	Shuffle	77.4	46.2	70.3	36.4
RAD (Inter)	80.9	51.0	73.9	40.3	Speed	80.9	51.0	73.9	40.3

shows that RAD (inter) is better than the simple trick proposed by [41] and RAD (intra), justifying our analysis in Sec. 3.1.

As also discussed in Sec. 3.1, reversing the frame order (Reverse), shuffling the frames (Shuffle), and changing video playback speed (Speed) are three commonly used tricks to break the motion information of a video. As shown by the comparison in Table 5 (right), Speed produces the best results, which is consistent with our analyses in Sec. 3.1. Reverse and Shuffle could change the motion feature of a video too aggressively, thus making the negative sample easy to be discriminated by the model.

Extra training strategies. Table 1 has shown that the two training strategies provide consistent improvements to MoQuad. We further validate the effectiveness of each strategy and the choice of the hyper-parameters in Table 6. The hard negative sampling mining and the warm-up with appearance task increase accuracy with proper hyper-parameters. To help better understand the warm-up strategy, we plot the ranking of different training samples from our quadruple in the pre-training process in Fig. 4. As shown in the left figure, the ranking of the Intra-Negs decreases with that of AD-Pos, implying the model first focuses on

Table 6. Ablation studies for the two extra training strategies. (Left) The hard negative sample mining strategy. $\beta = 0$ and $\alpha = 0$ is the best entry in Table 4(top). **(Right)** Appearance task warm-up. The entry of 0% is the best entry in the left sub-table. All models are pre-trained on UCF101 for 800 epochs.

β	α	Fine-tuning		Linear eval.		Warmup ratio	Fine-tuning		Linear eval.	
		UCF	HMDB	UCF	HMDB		UCF	HMDB	UCF	HMDB
0	0	80.9	51.0	73.9	40.3	0%	81.7	52.3	74.9	41.4
0.01	1.5	81.7	52.3	74.9	41.4	10%	82.8	53.0	75.6	42.0
0.01	2.0	81.5	51.6	74.8	41.6	20%	82.7	53.0	76.6	42.9
0.01	3.0	80.9	50.8	74.2	41.0	40%	81.0	50.8	74.2	40.8
0.05	1.5	79.3	49.7	72.7	40.3	60%	80.0	49.7	72.1	39.9

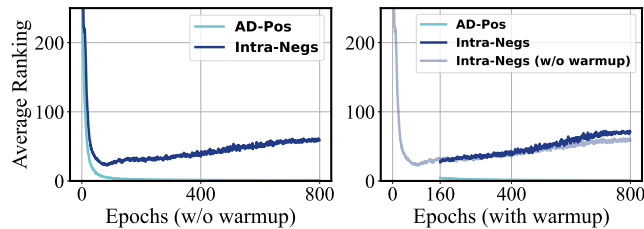


Fig. 4. Understanding the improvement brought by the warmup of appearance task. We plot the average rankings of the AD-Pos and the Intra-Negs. Intra-Negs includes Intra-Neg and the AD-Intra-Neg. Note that there are no Intra-Negs in the appearance task, thus we start plotting the right figure after the warm-up stage. The warm-up with the appearance task increases the average ranking of Intra-Negs.

the appearance of the video. While the right figure shows the warm-up strategy could increase the average ranking of the Intra-Negs during the training process. Note that a higher average ranking of Intra-Negs suggests that the model can better distinguish the subtle differences in motion information injected by the motion disturbing operation.

4.4 More analyses

Fine-grained action recognition results on SSv2. The paper’s motivation is to improve the motion learning for contrastive learning. To further verify if MoQuad indeed learns better motion feature, we extend the linear evaluation on the SSv2 dataset to a fine-grained split of video categories. As presented in Table 7, we compare MoQuad with our base method, SimCLR [7], on different categories, under the linear evaluation protocol. All the models are pre-trained on the training split of SSv2. MoQuad and SimCLR get similar performances for the top categories, but MoQuad significantly outperforms SimCLR on the bottom ones. Specifically, our method improves SimCLR by more than 40% on “Move something down”. Note that the bottom categories require accurate temporal features to be correctly recognized, indicating that MoQuad does teach the model to learn motion features better.

Table 7. Per-category accuracy on SSv2. We compare MoQuad with our base method, SimCLR [7], on fine-grained splits of SSv2 dataset to further demonstrate the capacity of our method to learn better motion features. The categories on the top can mostly be recognized using only the appearance information, while the bottom categories require deeper understanding of the motion in the video.

Video category in SSv2	SimCLR	MoQuad
Categories that do not need strong temporal information to classify		
Tear something into two pieces	75.2	83.9
Approach something with camera	60.1	88.9
Show something behind something	56.3	57.4
Plug something into two pieces	57.2	56.3
Hold something	27.4	26.3
Categories that need heavy temporal information to classify		
Move something and something closer	41.4	75.2
Move something and something away	29.2	74.5
Move something up	34.3	49.5
Move something down	24.3	68.6

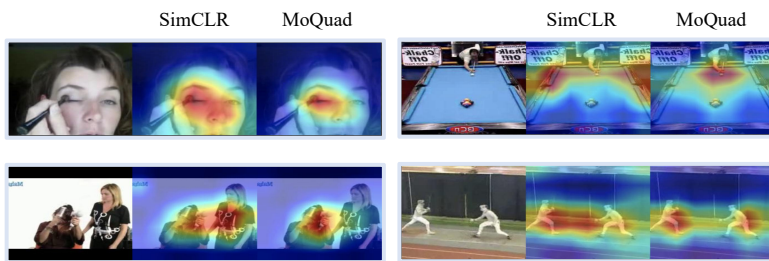


Fig. 5. Visualizing the region of interest (RoI). We use CAM [48] to plot the RoI of the model. MoQuad focuses more on the moving regions than SimCLR.

RoI visualization. We visualize the Region of Interest (RoI) of MoQuad and SimCLR in Fig. 5 using the tool provided by CAM [48]. Compared to SimCLR, MoQuad better constrains the attention to the moving regions, providing a clue that our method does improve the learning of motion-oriented features.

5 Conclusion

This paper proposes a simple yet effective method (MoQuad) to improve the learning of motion features in contrastive learning framework. A carefully designed sample construction strategy is the core of MoQuad, while two additional training strategies further improve the performance. By simply applying MoQuad to SimCLR, extensive experiments show that we outperform state-of-the-art self-supervised video representation learning approaches on both action recognition and video retrieval.

References

1. Agrawal, P., Carreira, J., Malik, J.: Learning to see by moving. 2015 IEEE International Conference on Computer Vision (ICCV) pp. 37–45 (2015) [4](#)
2. Benaim, S., Ephrat, A., Lang, O., Mosseri, I., Freeman, W., Rubinstein, M., Irani, M., Dekel, T.: Speednet: Learning the speediness in videos. 2020 IEEE/CVF Conference on Computer Vision and Pattern Recognition (CVPR) pp. 9919–9928 (2020) [10](#), [11](#)
3. Cai, T.T., Frankle, J., Schwab, D.J., Morcos, A.S.: Are all negatives created equal in contrastive instance discrimination? arXiv preprint arXiv:2010.06682 (2020) [5](#)
4. Caron, M., Bojanowski, P., Mairal, J., Joulin, A.: Unsupervised pre-training of image features on non-curated data. 2019 IEEE/CVF International Conference on Computer Vision (ICCV) pp. 2959–2968 (2019) [3](#)
5. Carreira, J., Zisserman, A.: Quo vadis, action recognition? a new model and the kinetics dataset. 2017 IEEE Conference on Computer Vision and Pattern Recognition (CVPR) pp. 4724–4733 (2017) [2](#), [8](#)
6. Chen, P., Huang, D., He, D., Long, X., Zeng, R., Wen, S., Tan, M., Gan, C.: Rspnet: Relative speed perception for unsupervised video representation learning. In: AAAI (2021) [2](#), [4](#), [6](#), [7](#), [9](#), [10](#), [11](#)
7. Chen, T., Kornblith, S., Norouzi, M., Hinton, G.: A simple framework for contrastive learning of visual representations. In: III, H.D., Singh, A. (eds.) Proceedings of the 37th International Conference on Machine Learning. Proceedings of Machine Learning Research, vol. 119, pp. 1597–1607. PMLR (13–18 Jul 2020), <https://proceedings.mlr.press/v119/chen20j.html> [1](#), [3](#), [9](#), [11](#), [13](#), [14](#)
8. Chen, X., He, K.: Exploring simple siamese representation learning. ArXiv [abs/2011.10566](#) (2020) [3](#)
9. Diba, A., Sharma, V., Gool, L., Stiefelhagen, R.: Dynamonet: Dynamic action and motion network. 2019 IEEE/CVF International Conference on Computer Vision (ICCV) pp. 6191–6200 (2019) [4](#)
10. Epstein, D., Chen, B., Vondrick, C.: Oops! predicting unintentional action in video. 2020 IEEE/CVF Conference on Computer Vision and Pattern Recognition (CVPR) pp. 916–926 (2020) [4](#)
11. Feichtenhofer, C., Fan, H., Malik, J., He, K.: Slowfast networks for video recognition. 2019 IEEE/CVF International Conference on Computer Vision (ICCV) pp. 6201–6210 (2019) [9](#)
12. Feichtenhofer, C., Fan, H., Xiong, B., Girshick, R.B., He, K.: A large-scale study on unsupervised spatiotemporal representation learning. 2021 IEEE/CVF Conference on Computer Vision and Pattern Recognition (CVPR) pp. 3298–3308 (2021) [2](#)
13. Gidaris, S., Singh, P., Komodakis, N.: Unsupervised representation learning by predicting image rotations. arXiv preprint arXiv:1803.07728 (2018) [3](#)
14. Goyal, R., Kahou, S.E., Michalski, V., Materzynska, J., Westphal, S., Kim, H., Haenel, V., Fründ, I., Yianilos, P.N., Mueller-Freitag, M., Hoppe, F., Thureau, C., Bax, I., Memisevic, R.: The “something something” video database for learning and evaluating visual common sense. 2017 IEEE International Conference on Computer Vision (ICCV) pp. 5843–5851 (2017) [8](#)
15. Grill, J.B., Strub, F., Altch’e, F., Tallec, C., Richemond, P.H., Buchatskaya, E., Doersch, C., Pires, B.Á., Guo, Z.D., Azar, M.G., Piot, B., Kavukcuoglu, K., Munos, R., Valko, M.: Bootstrap your own latent: A new approach to self-supervised learning. ArXiv [abs/2006.07733](#) (2020) [3](#)

16. Han, T., Xie, W., Zisserman, A.: Video representation learning by dense predictive coding. 2019 IEEE/CVF International Conference on Computer Vision Workshop (ICCVW) pp. 1483–1492 (2019) [2](#), [4](#), [9](#), [10](#)
17. Han, T., Xie, W., Zisserman, A.: Memory-augmented dense predictive coding for video representation learning. In: ECCV (2020) [4](#), [10](#), [11](#)
18. Han, T., Xie, W., Zisserman, A.: Self-supervised co-training for video representation learning. ArXiv [abs/2010.09709](#) (2020) [4](#), [10](#), [11](#)
19. Hara, K., Kataoka, H., Satoh, Y.: Can spatiotemporal 3d cnns retrace the history of 2d cnns and imagenet? 2018 IEEE/CVF Conference on Computer Vision and Pattern Recognition pp. 6546–6555 (2018) [8](#)
20. He, K., Fan, H., Wu, Y., Xie, S., Girshick, R.B.: Momentum contrast for unsupervised visual representation learning. 2020 IEEE/CVF Conference on Computer Vision and Pattern Recognition (CVPR) pp. 9726–9735 (2020) [1](#), [3](#)
21. He, T., Zhang, Z., Zhang, H., Zhang, Z., Xie, J., Li, M.: Bag of tricks for image classification with convolutional neural networks. In: Proceedings of the IEEE/CVF Conference on Computer Vision and Pattern Recognition. pp. 558–567 (2019) [9](#)
22. Hu, K., Shao, J., Liu, Y., Raj, B., Savvides, M., Shen, Z.: Contrast and order representations for video self-supervised learning. In: Proceedings of the IEEE/CVF International Conference on Computer Vision (ICCV). pp. 7939–7949 (October 2021) [4](#), [9](#), [11](#)
23. Huang, D., Wu, W., Hu, W., Liu, X., He, D., Wu, Z., Wu, X., Tan, M., Ding, E.: Ascnet: Self-supervised video representation learning with appearance-speed consistency. In: Proceedings of the IEEE/CVF International Conference on Computer Vision (ICCV). pp. 8096–8105 (October 2021) [2](#), [4](#), [9](#), [10](#), [11](#)
24. Huang, L., Liu, Y., Wang, B., Pan, P., Xu, Y., Jin, R.: Self-supervised video representation learning by context and motion decoupling. In: CVPR (2021) [10](#)
25. Isola, P., Zoran, D., Krishnan, D., Adelson, E.: Learning visual groups from co-occurrences in space and time. ArXiv [abs/1511.06811](#) (2015) [4](#)
26. Jayaraman, D., Grauman, K.: Learning image representations tied to ego-motion. 2015 IEEE International Conference on Computer Vision (ICCV) pp. 1413–1421 (2015) [4](#)
27. Jenni, S., Meishvili, G., Favaro, P.: Video representation learning by recognizing temporal transformations. ArXiv [abs/2007.10730](#) (2020) [6](#)
28. Jenni, S., Jin, H.: Time-equivariant contrastive video representation learning. In: Proceedings of the IEEE/CVF International Conference on Computer Vision (ICCV). pp. 9970–9980 (October 2021) [10](#)
29. Kolouri, S., Martin, C.E., Hoffmann, H.: Explaining distributed neural activations via unsupervised learning. 2017 IEEE Conference on Computer Vision and Pattern Recognition Workshops (CVPRW) pp. 1670–1678 (2017) [3](#)
30. Kuehne, H., Jhuang, H., Garrote, E., Poggio, T., Serre, T.: Hmdb: a large video database for human motion recognition. In: 2011 International conference on computer vision. pp. 2556–2563. IEEE (2011) [8](#)
31. Lai, Z., Lu, E., Xie, W.: Mast: A memory-augmented self-supervised tracker. 2020 IEEE/CVF Conference on Computer Vision and Pattern Recognition (CVPR) pp. 6478–6487 (2020) [4](#)
32. Luo, D., Liu, C., Zhou, Y., Yang, D., Ma, C., Ye, Q., Wang, W.: Video cloze procedure for self-supervised spatio-temporal learning. ArXiv [abs/2001.00294](#) (2020) [11](#)
33. Misra, I., Zitnick, C.L., Hebert, M.: Shuffle and learn: unsupervised learning using temporal order verification. In: European Conference on Computer Vision. pp. 527–544. Springer (2016) [6](#)

34. Noroozi, M., Favaro, P.: Unsupervised learning of visual representations by solving jigsaw puzzles. In: European conference on computer vision. pp. 69–84. Springer (2016) [3](#)
35. van den Oord, A., Li, Y., Vinyals, O.: Representation learning with contrastive predictive coding. ArXiv [abs/1807.03748](#) (2018) [3](#), [7](#)
36. Pan, T., Song, Y., Yang, T., Jiang, W., Liu, W.: Videomoco: Contrastive video representation learning with temporally adversarial examples. ArXiv [abs/2103.05905](#) (2021) [2](#), [10](#)
37. Qian, R., Li, Y., Liu, H., See, J., Ding, S., Liu, X., Li, D., Lin, W.: Enhancing self-supervised video representation learning via multi-level feature optimization. In: Proceedings of the IEEE/CVF International Conference on Computer Vision (ICCV). pp. 7990–8001 (October 2021) [10](#)
38. Qian, R., Meng, T., Gong, B., Yang, M.H., Wang, H., Belongie, S.J., Cui, Y.: Spatiotemporal contrastive video representation learning. In: CVPR (2021) [2](#), [4](#), [8](#), [9](#), [10](#), [11](#)
39. Soomro, K., Zamir, A.R., Shah, M.: A dataset of 101 human action classes from videos in the wild. Center for Research in Computer Vision **2**(11) (2012) [8](#)
40. Wang, J., Jiao, J., hui Liu, Y.: Self-supervised video representation learning by pace prediction. In: ECCV (2020) [2](#), [4](#), [6](#), [9](#), [10](#), [11](#)
41. Wang, J., Gao, Y., Li, K., Lin, Y., Ma, A.J., Sun, X.: Removing the background by adding the background: Towards background robust self-supervised video representation learning. In: CVPR (2021) [2](#), [4](#), [5](#), [6](#), [10](#), [12](#)
42. Wu, Z., Xiong, Y., Yu, S.X., Lin, D.: Unsupervised feature learning via non-parametric instance discrimination. In: Proceedings of the IEEE Conference on Computer Vision and Pattern Recognition. pp. 3733–3742 (2018) [3](#)
43. Xie, S., Sun, C., Huang, J., Tu, Z., Murphy, K.P.: Rethinking spatiotemporal feature learning: Speed-accuracy trade-offs in video classification. In: ECCV (2018) [8](#)
44. Xu, D., Xiao, J., Zhao, Z., Shao, J., Xie, D., Zhuang, Y.: Self-supervised spatiotemporal learning via video clip order prediction. 2019 IEEE/CVF Conference on Computer Vision and Pattern Recognition (CVPR) pp. 10326–10335 (2019) [11](#)
45. YM., A., C., R., A., V.: Self-labelling via simultaneous clustering and representation learning. In: International Conference on Learning Representations (2020), <https://openreview.net/forum?id=Hyx-jyBFPr> [3](#)
46. You, Y., Gitman, I., Ginsburg, B.: Large batch training of convolutional networks. arXiv preprint arXiv:1708.03888 (2017) [9](#)
47. Zhang, R., Isola, P., Efros, A.A.: Colorful image colorization. In: European conference on computer vision. pp. 649–666. Springer (2016) [3](#)
48. Zhou, B., Khosla, A., Lapedriza, A., Oliva, A., Torralba, A.: Learning deep features for discriminative localization. In: Computer Vision and Pattern Recognition (2016) [14](#)